MYOD1 Inhibits Avian Adipocyte Differentiation via miRNA-206/KLF4 Axis

Zheng Wang
China Agricultural University
Qiang-Sen Zhao
China Agricultural University
Xiao-Qin Li
China Agricultural University
Zhong-Tao Yin
China Agricultural University
Si-Rui Chen
China Agricultural University
Sen Wu
China Agricultural University
Ning Yang
China Agricultural University
Zhuo-cheng hou (zchou@cau.edu.cn)
China Agricultural University https://orcid.org/0000-0002-9506-612X

Research

Keywords: Avian, MYOD1, Adipocyte differentiation, CRISPR/CAS9, miR-206/KLF4 axis

Posted Date: November 19th, 2020

DOI: https://doi.org/10.21203/rs.3.rs-107745/v1

Version of Record: A version of this preprint was published at Journal of Animal Science and Biotechnology on May 5th, 2021. See the published version at https://doi.org/10.1186/s40104-021-00579-x.

Abstract

Background: A considerable number of muscle development-related genes were differentially expressed in the early stage of avian adipocyte differentiation. However, the functions of them in adipocyte differentiation remain largely known. In this study, the myoblast determination protein 1 (MYOD1) was selected as a representative of muscle development and we investigated its expression, function and regulation in avian adipocyte differentiation.

Results: The expression of MYOD1 decreased significantly in the early stage of avian adipocyte differentiation. CRISPR/CAS9-mediated deletion of MYOD1 induced adipocyte differentiation, whereas over-expression of MYOD1 inhibited adipogenesis. mRNA-seq showed that MYOD1 could perturb the lipid biosynthetic process during differentiation. Mechanistically, MYOD1 directly up-regulates the miR-206 expression by binding upstream 1200 bp region, and over-expression of miR-206 also inhibits adipogenesis. Furthermore, MYOD1 affected the expression of endogenous miR-206 and its target gene Kruppel Like Factor 4 (KLF4), which is an important activator of adipogenesis. Accordingly, the inhibition of miR-206 or over-expression of KLF4 could counteract the inhibitory effect of MYOD1 on adipocyte differentiation.

Conclusions: These findings suggest that MYOD1 inhibited adipocyte differentiation by up-regulating miR-206 to suppress the KLF4 expression. Collectively, these findings identify a novel function of MYOD1 in adipocyte differentiation, suggesting a potential role in body-fat distribution regulation.

Background

Adipocytes are unique in the quantity of lipids that they can store, the rapid release of these calories, and protein for use by other organs, which can profoundly affect our health [1]. Avian has been utilized as a good animal model for studying basic adipogenesis mechanisms, which can be directly used for genetic improvement of avian fat deposition [2]. Adipogenesis is driven by an increase in adipocyte cell size (hypertrophy) or number (hyperplasia) [3]. Adipocyte differentiation is regulated by an elaborate network of transcription factors, and understanding the underlying transcriptional networks is relevant and timely both from a basic and medical research perspective [4].

Several studies and observations showed fat deposits in the muscles will cause the loss of muscle quality and are more likely to induce metabolic diseases in various animals [5–8]. Adipose and muscle tissues originate from mesenchymal stem cells (MSCs) [9–12], which are the multipotent and relevant targets for therapies aiming to enhance tissue regeneration [13]. In response to lineage-specific inducers, MSCs from different depots can differentiate into many different, mutually exclusive lineages, including the adipocyte and myoblast lineages [14–16]. It has been shown that peroxisome proliferator-activated receptor γ (PPARγ) and myoblast determination protein 1 (MYOD1) are master regulators of adipogenesis and myogenesis, respectively [17, 18], and that the MYOD1-driven and PPARγ-driven differentiation programs are mutually exclusive [19–21]. However, the functional contributions of muscle development genes to adipocyte differentiation remain largely unexplored.

Our previous work found many muscle development genes involved in the early regulation of adipocyte differentiation [22]. In this study, MYOD1, a representative of muscle development, was significantly down-regulated in the early stage of avian adipocyte differentiation. Studies of loss-of-function and gain-of-function demonstrated that MYOD1 is a key repressor of adipocyte differentiation by interacting with miR-206/ Kruppel Like Factor 4 (KLF4) axis. The mRNA-seq showed that over-expression of MYOD1 in adipocytes inhibits the expression of most lipid biosynthesis genes and also promotes the expression of some myogenic genes. Our findings imply that a novel function of MYOD1 in adipocyte differentiation. Thus, affecting MYOD1 might represent a viable strategy to improve fat ratio to muscle in avian.

Materials And Methods

Plasmid construction`

MYOD1- Knock-out and Knock-in plasmids: Using the chMYOD1 sequence obtained from the NCBI database (Accession: NC_006092.5), we designed gRNA sequences targeting exon1 of chMYOD1, known as sgRNA1: CGACCCGTGCTTCAACACGT and sgRNA2: GCGGCTCAGCAAGGTCAACG. We synthesized the oligo-DNAs corresponding to these gRNAs. We annealed them to a T7 promoter-driven Cas9 and to a U6 promoter-driven gRNA vector in order to obtain two gRNA-expressing plasmids. In order to construct the MYOD1-over-expression vector, the full-length coding sequence of chMYOD1 (NCBI Reference Sequence: NM_204214.2) was amplified from chicken subcutaneous adipose cDNA by PCR, and cloned into the CMV promoter-driven piggyBac and an EF1α promoter-driven GFP plasmid by replacing GFP using EcoRI and SalI (New England Biolabs, Ipswich, MA, USA). Above plasmids were a gift from Professor Sen Wu (State Key Laboratory of Agrobiotechnology, College of Biological Sciences, China Agricultural University).

pmirGLO dual-luciferase reporters: The 3'-UTR fragment of KLF4 (NCBI Reference Sequence: XM_004949369.3) containing the binding sites were amplified by PCR from chicken subcutaneous adipose cDNA and then cloned into pmirGLO vector. The mutant vectors were constructed by PCR mutagenesis. Six seed sequences were successfully mutated from CATTCC to GTGAAG for the KLF4-3'-UTR vector.

Gene over-expression vector: The MYOD1 and KLF4 over-expression vector was constructed according to the user manual of the Easy Ligation Kit (Sidansai, Shanghai, China). MYOD1 and KLF4 coding sequence (NCBI Reference Sequence: NM_204214.2 and XM_004949369.3) were amplified from chicken subcutaneous adipose cDNA by PCR. The PCR product was cloned into the pcDNA3.1 vector. The successful MYOD1 and KLF4, over-expression vector, was confirmed by DNA sequencing.

miR-206 promoter reporter plasmid: A 1876 bp fragment of the miR-206 promoter was isolated by PCR using the primers listed in **Tab. S1**. After the PCR product was digested with KpnI and SmaI restriction sites, the insertion was ligated into the pGL4.1 vector (Promega, Madison, WI, USA) to create the expression vector pGL4.1(-1876). After pGL4.1(-1876) was sequenced, this construct was used as a template, and pGL4.1(-1234) was isolated by PCR. All cloning plasmids were confirmed by sequencing.

RNA extraction, cDNA synthesis, and quantitative real-time PCR

Total RNA was isolated from the cells using RNAiso reagent (Takara, Otsu, Japan) according to the manufacturer's instruction. According to the manufacturer's manual, the reverse transcription reaction for mRNA was performed with PrimeScript RT reagent Kit (Perfect Real-Time) (Takara, Otsu, Japan). The reverse transcription reaction for miRNA was using miRNA First-Strand cDNA Synthesis SuperMix (Transgen, Beijing, China). The specific qRT-PCR Primer of mRNA and miRNA were designed using Primer 3 software (version 0.4.0, Howard Hughes Medical Institute). Primer sets are listed in **Tab. S1**. With KAPA SYBR FAST qPCR Kit (KAPA Biosystems, MA, USA), qPCR program was carried out in ABI-7500 PCR machine (Applied Biosystems, MA, USA), and the method was as described [23]. All reactions were run in triplicate.

Cell culture

A cell line of immortalized chicken preadipocytes (ICPs) [24] was a kind gift of the Poultry Breeding Group of the College of Animal Science and Technology, Northeast Agricultural University, and was cultured in DMEM/F12 (Gibco, Gaithersburg, MD, USA) supplemented with 10% fetal bovine serum (Hyclone, Logan, UT, USA), and 0.2% penicillin/streptomycin (Invitrogen, Carlsbad, CA, USA). To induce ICPs differentiation, we added 160 μM sodium oleate (Sigma Life Science, St. Louis, MO, USA) to the medium [25].

For MYOD1^{OE} and MYOD^{KO} cells selection, ICPs were seeded in 6-well plates for further transfection using Lipofectamine 3000 (Invitrogen, Carlsbad, CA, USA). After a 48 h recovery period, the cells were supplemented with 3 μg/mL of puromycin (Sigma-Aldrich, MO, USA) in the culture medium for 12 days until clone formation. Cells were harvested using 0.25% trypsin/EDTA (Gibco, Gaithersburg, MD, USA), and the cell density was calculated using a handheld automated cell counter (Millipore, Darmstadt, Germany). Single cells were plated in each well of a 96-well plate by limiting dilution and then cultured for 10 d in the cell culture medium. The medium was replaced every 4 d. Confluent cell colonies were propagated and genotyped by PCR and sequencing.

Transfections

Transfections were performed with Lipofectamine 3000 reagent (Invitrogen, Carlsbad, CA, USA) according to the manufacturer's direction. Nucleic acids were diluted in OPTI-MEM Medium (Gibco, Gaithersburg, MD, USA). All experiments were carried out at least three times independently.

Oil Red O staining and quantification

The cells were washed with PBS and fixed in 4% formaldehyde for 10 min. Then the cells were stained with Oil-Red-O working solution (Solarbio, Beijing, China) according to the manufacturer's manual. After another wash with PBS, the cell nuclei were counterstained with Hoechst 33342 (Solarbio, Beijing, China). Morphological changes were observed and photographed under an inverted fluorescent microscope (Nikon). The Oil-Red-O dyes were then extracted in isopropanol solution containing 4% Nonidet P-40 and quantified by NanoDrop 2000C spectrophotometers (Thermo Fisher Scientific, San Jose, CA, USA) at 510 nm.

RNA oligonucleotides

The miR-206 mimics, negative control (NC) mimic, miR-206 inhibitors and NC inhibitor were all purchased from GenePharma (GenePharma, Shanghai, China).

Dual-luciferase reporter assay

For the promoter activity assays, ICPs were cotransfected with reporter plasmid and MYOD1 over-expression vector or control vector, and the TK-Renilla reporter was also cotransfected to each sample as an internal control using the Lipofectamine 3000 reagent (Invitrogen, Carlsbad, CA, USA) in 48-well plates. The miRNA target verification assay was also performed in ICPs. Wild-type or mutant KLF4-3'-UTR dual-luciferase reporter (200 ng) and miR-206 mimic or NC mimic (50 nM) were cotransfected into ICPs. After 48 h transfection, cells were washed by PBS twice, and the activities of Firefly and Renilla luciferase were measured according to the manual of Luc-pair Duo-Luciferase Assay Kit 2.0 (GeneCopoeia, Rockville, MD, USA). All the data were acquired by averaging the results from three independent repeats.

Western blot

Cultured cells were washed with PBS and homogenized with RIPA buffer (Beyotime, Jiangsu, China) containing protease inhibitor cocktail (Beyotime, Jiangsu, China). Protein concentrations were determined using the BCA Protein Assay Kit (Beyotime, Jiangsu, China). Proteins were denatured and subjected to 10% polyacrylamide gel and transferred to methanol-activated PVDF membranes. Blots were probed using the primary antibodies: mouse anti-MYOD1 (1:500; Santa Cruz Biotechnology, USA, Cat# sc-377460), rabbit anti-KLF4 (1:500; Bioss, Beijing, China, Cat# 52850R), mouse anti-GAPDH, (1:5000; Bioworld, St Louis Park, MN, USA, Cat#MB001), overnight at 4 °C. After one h incubation with anti-mouse or anti-rabbit HRP-conjugated second antibody (1:5000, Bioss, Beijing, China, Cat# 40296G, 40295G). Immunodetection was performed using enhanced chemiluminescence (ECL) Western blotting substrate (Beyotime, Jiangsu, China) and detected with FluoChem R imaging system (ProteinSimple, CA, USA).

RNA-seq analysis

Raw reads were trimmed to remove adapters and low-quality reads, with Trimmomatic (version 0.39) [26]. Trimmed reads were mapped to the chicken reference genome (Ensembl release 100:ftp://ftp.ensembl.org/pub/release100/fasta/gallus_gallus/dna/Gallus_gallus.GRCg6a.dna.toplevel.fa.gz) using HISAT2[27]. Read counts for each gene were calculated using Stringtie (v.2.1.2) and normalized by library sequencing depth using the R package DESeq2 (v.1.28.1) after filtering the gene with low expression [28]. We used the DEGSeq2 (v.1.28.1) package to identify DEGs between $MYOD1^{NC}$, $MYOD1^{KO}$, and $MYOD1^{OE}$ cells at different days (day 0 and day 5). Therefore, samples were excluded from further analysis due to its low global Pearson correlation with the other repeat samples ($R^2 < 0.95$). Genes with $|log2FC| \geq 0.585$ (or ≥ 1) and the Benjamini□Hochberg (BH) adjusted p-value (adjusted-P value) < 0.05 were considered as differentially expressed genes.

Functional enrichment and prediction of miRNA target genes

Genes were annotated with gene Symbols from the Uniprot database for functional annotation. Gene ontology (GO) analysis of the enriched genes was performed using the web-based Metascape [29] (a gene annotation & analysis resource, http://metascape.org/gp/index.html#/main). Putative miRNA targets for miR-206 were predicted by online software, TargetScan (version 7.2, http://www.targetscan.org/), miRDB (http://mirdb.org/) as well as miRTarBase (http://mirtarbase.cuhk.edu.cn/) to choose target genes for validation.

Statistical analysis.

Each experiment was repeated three times, and all results are represented as the mean ± SD. Three independent sample t-test was used to perform the statistically significant difference between groups. The level of significance was presented as $*$ ($p < 0.05$).

Results

MYOD1 is a repressor of adipocyte differentiation

We found that the expression of MYOD1 is significantly down-regulated after the beginning of Pekin duck adipocyte differentiation (Fig. 1a). To further understand the relationship between MYOD1 and adipocyte differentiation, we detected its expression in adipogenic differentiation of immortalized chicken preadipocytes (ICPs) by qPCR (Fig. 1b) and Western blot (Fig. 1c). MYOD1 was also significantly down-regulated its expression after adipocyte differentiation in chicken. These results indicate that MYOD1is involved in the avian adipocyte differentiation process.

To further determine the roles of MYOD1 in avian adipocyte differentiation, we first performed gain-of-function experiments by using piggyBack delivery [30] of MYOD1 into ICPs. As shown in Fig. 2a and b, transduced MYOD1 clone can significantly induce MYOD1 expression relative to cells transduced with a control vector. Strikingly, over-expression of MYOD1 in ICPs ($MYOD1^{OE}$) significantly blocked adipogenesis (Fig. 2c, d), as shown by oil red O staining of neutral lipids. Adipocyte markers, such as PPARγ, A-FABP, C/EBPα,and C/EBPβ (Fig. 2e), were significantly decreased in $MYOD1^{OE}$ cells.

We further sought confirmation of MYOD1 anti-adipogenic activity through loss-of-function studies, in which we would predict enhanced adipose conversion. We transfected ICPs with two single guide RNAs (sgRNAs) targeting the exon 1 of MYOD1 and a Cas9 vector. We established MYOD1-knock-out ICP Clones ($MYOD1^{KO}$) with a 260-bp frame-shifting deletions in MYOD1 (Fig. 2f), indicating that both gRNAs work efficiently with Cas9 to edit MYOD1. The mutation of MYOD1 also dramatically down-regulated its expression relative to cells transfected with an only Cas9 vector (Fig. 2g, h). $MYOD1^{KO}$ cells demonstrated enhanced adipogenic potential, including greater lipid accumulation (Fig. 2i, j), and increased the expression of adipocyte marker genes (Fig. 2k).

MYOD1 perturb the lipid biosynthetic process

To further understand the effect of MYOD1 on adipogenesis, we performed mRNA-Seq experiments in $MYOD1^{OE}$, $MYOD1^{NC}$, $MYOD1^{KO}$ cells prior to differentiation (day 0) and day 5 after differentiation. In total, 886 and 1335 differentially expressed genes (DEGs) were up-regulated and down-regulated in $MYOD1^{OE}$ cells compared to $MYOD1^{NC}$ cells on day 0, respectively (Tab. S2, Fold-Change > 2; adjusted-*P* value < 0.05). GO analysis for DEGs up-regulated in $MYOD1^{OE}$ cells are enriched for development processes such as blood vessel development, muscle structure development, and positive regulation of muscle tissue development, while DEGs down-regulated in $MYOD1^{OE}$ cells are enriched for extracellular matrix organization, metabolism process, and cell morphogenesis involved in differentiation (Table 1, Tab. S3). Also, 256 and 971 DEGs were up-regulated and down-regulated in $MYOD1^{KO}$ cells compared to $MYOD1^{NC}$ cells on day 0, respectively (Tab. S2, Fold-Change > 2; adjusted-*P* value < 0.05). As expected, GO analysis for genes down-regulated in $MYOD1^{KO}$

cells also are enriched for striated muscle cell differentiation and muscle system process. In contrast, genes up-regulated in MYOD1^{KO} cells are enriched in the adipogenesis related pathway, including cell morphogenesis in differentiation, regulation of MAPK cascade, and positive regulation of lipid metabolic process (Table 1, Tab. S3). These results indicate that although differentiation has not yet begun, the knock-in or knockout of MYOD1 alone seems to have affected preadipocytes characteristics.

Table 1

GO enrichment analysis of DEGs in $MYOD1^{OE}$, $MYOD1^{NC}$, and $MYOD1^{KO}$ cells

	Up-regulated	Gene count	Log (q-value)	Down-regulated	Gene count	Log (q-value)
$MYOD1^{OE}$ VS $MYOD1^{KO}$ (Day 0)	blood vessel development	74	-11.19	cell involved in differentiation	25	-1.35
	muscle structure development	64	9.51	extracellular matrix organization	38	-1.35
	heart development	56	-8.84	ATP metabolic process	21	-1.35
	actin cytoskeleton organization	60	-7.72	inorganic cation transmembrane transport	36	-1.12
	muscle tissue development	41	-6.50	developmental growth	30	-0.66
$MYOD1^{KO}$ VS $MYOD1^{NC}$ (Day 0)	regulation of cell morphogenesis	18	-3.09	regulation of system process	44	-8.02
	positive regulation of cell development	17	-2.34	skeletal system development	35	-5.05
	cell involved in differentiation	19	-2.19	muscle structure development	37	-3.82
	regulation of MAPK cascade	18	– 1.89	heart development	34	-3.82
	regulation of lipid metabolic process	11	-1.09	muscle system process	29	-3.66
$MYOD1^{OE}$ Day 5 VS Day 0	nuclear division	70	-13.19	actin cytoskeleton organization	146	-23.46
	ncRNA metabolic process	78	-10.61	heart development	128	-21.58
	DNA replication	48	-9.70	skeletal system development	118	-20.87
	regulation of cell cycle process	83	-5.79	extracellular structure organization	95	-16.49
	ribosomal large subunit biogenesis	17	-4.12	muscle structure development	126	-15.92
$MYOD1^{NC}$ Day 5 VS Day 0	nuclear division	59	– 21.11	extracellular matrix organization	46	-11.38
	cell division	71	-21.11	heart development	52	-8.01
	lipid biosynthetic process	40	-2.74	muscle structure development	55	-7.35

	Up-regulated	Gene count	Log (q-value)	Down-regulated	Gene count	Log (q-value)
	regulation of MAPK cascade	36	-1.33	skeletal system development	45	-6.29
	glycerophospholipid metabolic process	19	-1.72	regulation of lipid metabolic process	35	-4.68
$MYOD1^{KO}$ Day 5 VS Day 0	cell division	68	-6.78	extracellular structure organization	66	-8.36
	protein autophosphorylation	22	-4.05	DNA replication	44	-4.73
	mitotic nuclear division	46	-4.02	skeletal system development	61	-3.78
	lipid biosynthetic process	40	-2.74	phospholipid metabolic process	53	-3.78
	regulation of cell cycle process	64	-2.13	muscle structure development	56	-0.89

To better understand the effect of MYOD1 on adipogenesis, we re-analyzed the DEGs before and after adipogenic differentiation in $MYOD1^{KO}$, $MYOD1^{NC,}$ and $MYOD1^{OE}$ cells. A total of 2457, 781, and 1636 DEGs were significantly up-regulated on day 5 of differentiation of $MYOD1^{OE}$, $MYOD1^{NC,}$ and $MYOD1^{KO}$ cells compared to day 0, respectively (Tab. S4, Fold-Change > 1.5; adjusted-*P* value < 0.05). The up-regulated DEGs of the three adipocyte lines on day 5 were significantly enriched in cell division and DNA replication, which is an essential step in adipocyte differentiation. At the same time, down-regulated DEGs are also significantly enriched in muscle structure development (Table 1, Tab. S5), indicating that muscle development-specific genes are also considerably suppressed during chicken adipocyte differentiation. Notably, we found that the lipid biosynthetic process was only enriched in the DEGs up-regulated on day 5 in $MYOD1^{KO}$ and $MYOD1^{NC}$ cells, but not in $MYOD1^{OE}$ cells (Table 1, Tab. S5). Furthermore, to test whether MYOD1 over-expression impacts the lipid biosynthetic process in a statistical threshold-independent manner, we directly compared expression fold-changes of known lipid biosynthesis genes (from Genecards database: Pathcards: Fatty Acyl-CoA Biosynthesis & Triglyceride Biosynthesis) during adipocyte differentiation and found that most lipid biosynthesis genes tended to be up-regulated on day 5 of $MYOD1^{KO}$ cells, but down-regulated in $MYOD1^{OE}$ cells (Fig. 2l, Tab. S6), which consistent with observations from our phenotype-profiling experiments and indicating that MYOD1 is a repressor for the adipogenesis.

The expression of miR-206 can be significantly induced in $MYOD1^{OE}$ cells

MYOD1 has been confirmed to induce highly conserved muscle-specific microRNAs (myomiRs) expression by binding to miRNA upstream regions, including miR-1, miR-133a, miR-133b, and miR-206, and these myomiRs are widely directly involved in the inhibition of other pathways [31–35]. qPCR assay found that $MYOD1^{OE}$ cells

expressed significantly higher levels of miR-1, miR-133a, miR-133b, and miR-206 (Fig. 3a), and miR-206 has the highest expression fold change (≈ 40 fold). MYOD1^{KO} cells also significantly reduce miR-206 expression (Fig. 3b). Also, we found multiple binding sites of MYOD1 in the 2000 bp upstream region of gga-miR-206, especially within 1200 bp (Tab. S7). Thus, we hypothesize that miR-206 may be an essential mediator for MYOD1 to inhibit adipocyte differentiation. To validate the regulatory relationship between MYOD1 and miR-206 transcription, two distinct lengths of upstream regions (1876 and 1234 bp) of the gga-miR-206 transcription start site were amplified and cloned into pGL4.10 vector to detect the promoter activity. After cotransfecting with pGL-TK and pcNA3.1-MYOD1 into ICPs, both of pGL4.1(− 1876 bp) and pGL4.1(− 1234 bp) showed a significantly increasing promoter activity compared to cotransfected with pGL-TK and pcNA3.1 ($p < 0.05$) (Fig. 3c). Our results showed that the chicken MYOD1 can bind to 1200 bp upstream region of gga-miR-206 and promote the transcription activity of miR-206 in ICPs, as previously reported [36].

miR-206 is a downstream gene of MYOD1 that inhibits adipocyte differentiation

We then examined the expression and function of miR-206 during adipocyte differentiation. The expression of miR-206, similar to the protein level of MYOD1, was significantly down-regulated after differentiation (Fig. 3d), suggesting a synergistic relationship between them, and both of them were involved in this process. Therefore, we transfected miR-206 mimic and inhibitor into ICPs, respectively. Transfection-mediated gene transfer resulted in up to 840-fold elevation in the expression of miR-206 (Fig. 3e). Over-expression of miR-206 also significantly inhibits lipid droplet accumulation and reduced adipocyte marker genes expression (Fig. 3f, g), whereas the inhibition of miR-206 promotes adipocyte differentiation (Fig. 3h-j). Together, these results demonstrated that miR-206 could inhibit adipocyte differentiation.

To examine whether MYOD1 targets miR-206 to regulate adipocyte differentiation, we transfected MYOD1^{OE} cells with miR-206 inhibitor and knock-down of miR-206 could counteract the inhibition effect of MYOD1 over-expression on adipocyte differentiation (Fig. 3k, l). Similarly, over-expression of miR-206 also significantly inhibited lipid accumulation in MYOD1^{KO} cells (Fig. S1a-c). Together, these results suggest that the inhibitory effect of MYOD1 on adipocyte differentiation was achieved by its downstream gene miR-206.

KLF4 is a miR-206 target gene, functioning as an activator of adipocyte differentiation

In order to explore the potential mechanism of miR-206 in regulating adipocyte differentiation, we performed bioinformatic analysis. Three bioinformatic tools (TargetScan, miRDB, and miRTarBase) were employed to identify the candidate targets of miR-206 (Tab. S8). All three programs predicted a total of 16 miR-206 target genes, such as KLF4, CCND2, and UTRN (Fig. 4a). Among them, we noticed that KLF4, a key activator of adipocyte differentiation, contains the miR-206 binding site in its 3'-UTR (Fig. 4b). This binding site is conserved among avian (Fig. 4c), suggesting the biological relevance of miR-206 in regulating KLF4 expression in avian. mRNA-seq also showed that the fold change (day 5 vs. day 0) of KLF4 expression was the highest in the differentiated MYOD1^{KO} cells, followed by the MYOD1^{NC}, and the lowest in the MYOD1^{OE} cells (Fig. 4d). To validate whether KLF4 is the target gene of miR-206, the 3′-UTR of chicken KLF4 containing

the wild-type or mutated miR-206-binding sites were cloned into pmirGLO vector, and the luciferase activity was found to be significantly decreased in ICPs cotransfected with the vector carrying the wild-type-binding site in the presence of miR-206 mimics, but not in ICPs carrying the mutated-binding site (Fig. 4e). On the other hand, the luciferase activity was found to be significantly increased in ICPs cotransfected with the vector carrying the wild-type-binding site in the presence of miR-206 inhibitor, but not in ICPs carrying the mutated-binding site (Fig. 4f). In addition, over-expression of miR-206 inhibited the mRNA and protein level of KLF4 (Fig. 4g, h), and the inhibition of miR-206 promoted the mRNA and protein level of KLF4 (Fig. 4i, j). Therefore, the above results indicated that KLF4 is the miR-206 target gene.

During adipocyte differentiation, KLF4 mRNA has gradually up-regulated its expression until day 3 (Fig. 4k). However, the protein level for KLF4 reached the highest on the day 1 after differentiation and disappeared on day 3 (Fig. 4l). Our results, as the previous report, showed that KLF4 was induced very early following the induction of adipogenesis, and function as an early regulator of adipocyte development has been attributed to its capacity to induce C/EBPβ expression [37, 38]. Furthermore, we cotransfected miR-206 and pcDNA3.1-KLF4 into ICPs, and KLF4 over-expression is able to counteract the inhibition effect of miR-206 on adipocyte differentiation (Fig. 4m, n). Therefore, KLF4 is the miR-206 target gene, which can function as an activator of adipocyte differentiation.

Based on the above results, we can deduce MYOD1 inhibits adipocyte differentiation by inhibiting the expression of KLF4. Western blot show MYOD1^{KO} cells expressed significantly higher protein levels of KLF4, while MYOD1^{OE} cells expressed lower protein levels of KLF4 (Fig. 5a). Finally, over-expression of KLF4 also significantly promoted adipocyte differentiation in MYOD1^{OE} cells (Fig. 5b, c). In addition, over-expression of MYOD1 could significantly inhibit the expression of KLF4's target genes C/EBPβ, while inhibiting miR-206 or over-expression of KLF4 in MYOD1^{OE} cells will significantly increase C/EBPβ expression.

Discussion

Avian are important farm animals throughout the world, producing eggs and high-quality meat for humans. Muscle mass and fat content are both important traits for meat-producing chickens but attaining an appropriate muscle and fat ratio is an excellent challenge for the broiler industry [39]. Discovering functional genes that can simultaneously regulate muscle and adipocyte development is a key step to improve these traits [40]. Previous and current transcriptomic data have shown that many muscle development genes were differentially expressed during adipocyte differentiation. Among these, our study investigated MYOD1 inhibited avian adipocyte differentiation via the miRNA-206/KLF4 axis (Fig. 5d). We have also identified a negative regulation between MYOD1 and lipid biosynthesis genes during adipogenesis. Previous studies reported that MYOD1 expression in brown fat is significantly reduced, and it inhibits brown fat development through PRDM16 [41]. A lineage-tracing study reveals that the MYOD1 lineage does not give rise to brown adipocytes, indicating a role of MYOD1 in myogenic cell fate switch in the common progenitors that give rise to both myoblasts and brown preadipocytes [20]. Moreover, the loss of MYOD1 also facilitates the adipogenic trans-differentiation of C2C12 myoblasts by the miR-133/IGF1R/PI3K/AKT signaling pathway [35]. These findings revealed a novel function of MYOD1 in adipogenesis.

MYOD1 is considered as a master regulator of myogenesis as its expression can induce myogenic differentiation in myoblasts, fibroblasts, and a variety of other cell types [18, 42, 43].In this study, muscle structure development was significantly enriched in the up-regulated DEGs of $MYOD1^{OE}$ cells, and also enriched in down-regulated DEGs of $MYOD1^{KO}$ on day 0, which all demonstrate the strong transcriptional regulatory activity of MYOD1 on downstream genes. Whether the ectopic expression of MYOD1 in preadipocytes promoted the myogenesis has not been examined in this study. Still, this evidence makes us believe that the over-expression of MYOD1 can promote the trans-differentiation of preadipocytes into muscle cells. In addition, several co-culture experiments have revealed that adipogenesis is strongly inhibited by the presence of satellite cell-derived myofibres [8, 44]. Supportively, the transcriptomic analysis also suggested that MYOD1 would be a repressor of adipogenesis by inhibiting the expression of lipid biosynthesis genes. Similarly, myogenesis was wholly blocked in both the MYOD1/MYF5 and MYOD1/IGF2 double knockout mice. Both results showed potential functions of MYOD1 on adipogenesis [45, 46]. On the other hand, myoblasts trans-differentiate into mature adipocytes by ectopic expression of adipogenic transcription factors under conditions permissive for adipogenesis [14]. The mutual exclusion of the two lineage-specific transcription factors balances and determines the developmental separation of fat and muscle tissue.

The current fast-growing and high-energy diet makes the chicken more likely to show myopathy, such as white striping, characterized by more fat in the breast muscles, resulting in meat with higher fat content and lower protein content [47, 48]. Combined with previously reported that MYOD1 can promote muscle development, increasing the expression of MYOD1 may be an effective strategy to treat these diseases.

Finally, we show that miR-206 is an important mediator of MYOD1 induced inhibition of adipogenesis. The miR-206 is one of the most studied miRs thus far, and it has also been confirmed to be involved in the pathogenesis of many diseases, including heart failure, chronic obstructive pulmonary disease, and various types of cancers [49, 50]. In chicken, miR-206 is significantly associated with broiler birthweight [36]. Various TFs essential for skeletal muscle development have been shown to regulate miR-206 expression during myogenic differentiation, such as MYF5, MYOD1, MYOG, and MEF2C [51–53]. In mammals, miR-206 promotes apoptosis, induce cell cycle arrest, and inhibit cell migration and adipocyte differentiation by targeting c-Met and its downstream PI3K/AKT pathway [54, 55]. Through TargetScan and miRDB analysis, however, c-MET was not the target gene of gga-miR-206 (Tab. S8). And the potential binding site of gga-miR-206 is also not in the 3'-UTR of c-Met (Tab. S9), which may be due to a divergence in evolution. KLF4 has been shown to be induced very early following the induction of adipogenesis, and knock-down of KLF4 inhibits adipogenesis [37]. The ability of KLF4 to function as an early regulator of adipocyte development has been attributed to its capacity to induce C/EBPβ expression [37]. C/EBPβ, an important early factor of adipogenesis, is responsible for inducing C/EBPα and PPARγ, which are the two master transcription factors for terminal adipocyte differentiation [56, 57]. Indeed, in this study, we found that C/EBPβ, C/EBPα, and PPARγ were significantly inhibited in $MYOD1^{OE}$ cells than in $MYOD1^{NC}$, but they were increased after over-expression of KLF4 or inhibition of miR-206, suggesting a possible involvement of KLF4 and C/EBPβ in the inhibition of MYOD1 on C/EBPα and PPARγ transcription.

Conclusions

In summary, this study provides a new insight into that MYOD1 also works as the repressor of adipocyte differentiation via miR-206/KLF4 axis in avian adipocyte model. Considering the significant role of adipocyte differentiation in the formation and function of adipose, clarification of the mechanism of MYOD1-mediated regulation of adipocyte differentiation is essential for exploring strategies for the treatment of metabolic disorders, including white striping. In combination with previous findings of the beneficial role of MYOD1 in muscle differentiation, we proposed that MYOD1 may be a crucial target for improving the ratio of muscle to fat in avian.

Abbreviations

A-FABP: Fatty Acid Binding Protein 4; C/EBPs: CCAAT Enhancer Binding Proteins; CDS: Coding sequence; c-MET: MET Proto-Oncogene, Receptor Tyrosine Kinase; CRISPR: Clustered Regularly Interspaced Short Palindromic Repeats; DEGs: Differentially expressed unigenes; FBS: Foetal bovine serum; GO: Gene Ontology; KLF4: Kruppel Like Factor 4; MYOD1: Myogenic Differentiation 1; PPARγ: Peroxisome Proliferator Activated Receptor Gamma; RT-qPCR: Quantitative real-time PCR; RNA-Seq: High-throughput sequencing of RNA; UTR: Untranslated region

Declarations

Acknowledgements

We thank the Poultry Breeding Group of the College of Animal Science and Technology, Northeast Agricultural University, for providing the ICPs line.

Funding

The work was supported by the National Waterfowl-Industry Technology Research System (CARS-42), National Nature Science Foundation of China (31972525, 31572388), Beijing Municipal Science & Technology Commission (Z181100002418008), Key-Area Research and Development Program of Guangdong Province (2020B020222003).

Availability of data and materials

The data analyzed during the current study are available from the corresponding author on reasonable request.

Authors' contributions

ZCH conceived and designed the experimental plan. ZW, XQL and SRC collected samples and performed the experiments. ZW, QSZ and ZTY participated in bioinformatics analyses. ZW, QSZ, NY and ZCH drafted and revised this manuscript. All authors read and approved the final manuscript.

Ethics statement

Collection of adipose samples for use in the described experiments were conducted following methods approved by the Animal Care and Use Committee of China Agricultural University (permit number: SYXK 2007–0023).

Consent for publication

Not applicable.

Competing interests

The authors declare that they have no competing interests.

Author details

Department of Animal Genetics and Breeding, College of Animal Science and Technology, China Agricultural University, Beijing 100193, China.

State Key Laboratory of Agrobiotechnology, College of Biological Sciences, China Agricultural University

References

1. Ghaben AL, Scherer PE. Adipogenesis and metabolic health. Nat Rev Mol Cell Biol. 2019;20(4):242–58.
2. Abdalla BA, Chen J, Nie Q, Zhang X. Genomic Insights Into the Multiple Factors Controlling Abdominal Fat Deposition in a Chicken Model. Front Genet. 2018;9:262.
3. Wang QA, Tao C, Gupta RK, Scherer PE. Tracking adipogenesis during white adipose tissue development, expansion and regeneration. Nat Med. 2013;19(10):1338–44.
4. Lee JE, Schmidt H, Lai B, Ge K. **Transcriptional and Epigenomic Regulation of Adipogenesis**. Mol Cell Biol. 2019; 39(11).
5. Longo M, Zatterale F, Naderi J, Parrillo L, Formisano P, Raciti GA, et al. **Adipose Tissue Dysfunction as Determinant of Obesity-Associated Metabolic Complications**. Int J Mol Sci. 2019; 20(9).
6. Kusminski CM, Bickel PE, Scherer PE. Targeting adipose tissue in the treatment of obesity-associated diabetes. Nat Rev Drug Discov. 2016;15(9):639–60.
7. Sihvo HK, Immonen K, Puolanne E. Myodegeneration with fibrosis and regeneration in the pectoralis major muscle of broilers. Vet Pathol. 2014;51(3):619–23.
8. Uezumi A, Fukada S, Yamamoto N, Takeda S, Tsuchida K. Mesenchymal progenitors distinct from satellite cells contribute to ectopic fat cell formation in skeletal muscle. Nat Cell Biol. 2010;12(2):143–52.
9. Cristancho AG, Lazar MA. Forming functional fat: a growing understanding of adipocyte differentiation. Nat Rev Mol Cell Biol. 2011;12(11):722–34.
10. Cawthorn WP, Scheller EL, MacDougald OA. Adipose tissue stem cells meet preadipocyte commitment: going back to the future. J Lipid Res. 2012;53(2):227–46.
11. Liu TM, Martina M, Hutmacher DW, Hui JH, Lee EH, Lim B. Identification of common pathways mediating differentiation of bone marrow- and adipose tissue-derived human mesenchymal stem cells into three mesenchymal lineages. Stem Cells. 2007;25(3):750–60.

12. Rauch A, Haakonsson AK, Madsen JGS, Larsen M, Forss I, Madsen MR, et al. Osteogenesis depends on commissioning of a network of stem cell transcription factors that act as repressors of adipogenesis. Nat Genet. 2019;51(4):716–27.
13. Squillaro T, Peluso G, Galderisi U. Clinical Trials With Mesenchymal Stem Cells: An Update. Cell Transplant. 2016;25(5):829–48.
14. Hu E, Tontonoz P, Spiegelman BM. Transdifferentiation of myoblasts by the adipogenic transcription factors PPAR gamma and C/EBP alpha. Proc Natl Acad Sci U S A. 1995;92(21):9856–60.
15. Jiang J, Li P, Ling H, Xu Z, Yi B, Zhu S. MiR-499/PRDM16 axis modulates the adipogenic differentiation of mouse skeletal muscle satellite cells. Hum Cell. 2018;31(4):282–91.
16. De Coppi P, Milan G, Scarda A, Boldrin L, Centobene C, Piccoli M, et al. Rosiglitazone modifies the adipogenic potential of human muscle satellite cells. Diabetologia. 2006;49(8):1962–73.
17. Rosen ED, Sarraf P, Troy AE, Bradwin G, Moore K, Milstone DS, et al. PPAR gamma is required for the differentiation of adipose tissue in vivo and in vitro. Mol Cell. 1999;4(4):611–7.
18. Davis RL, Weintraub H, Lassar AB. Expression of a single transfected cDNA converts fibroblasts to myoblasts. Cell. 1987;51(6):987–1000.
19. Singh J, Verma NK, Kansagra SM, Kate BN, Dey CS. Altered PPARgamma expression inhibits myogenic differentiation in C2C12 skeletal muscle cells. Mol Cell Biochem. 2007;294(1–2):163–71.
20. Sanchez-Gurmaches J, Guertin DA. Adipocytes arise from multiple lineages that are heterogeneously and dynamically distributed. Nat Commun. 2014;5:4099.
21. Sunadome K, Suzuki T, Usui M, Ashida Y, Nishida E. Antagonism between the master regulators of differentiation ensures the discreteness and robustness of cell fates. Mol Cell. 2014;54(3):526–35.
22. Wang Z, Yin ZT, Zhang F, Li XQ, Chen SR, Yang N, et al. Dynamics of transcriptome changes during subcutaneous preadipocyte differentiation in ducks. BMC Genom. 2019;20(1):688.
23. Livak KJ, Schmittgen TD. Analysis of relative gene expression data using real-time quantitative PCR and the 2(-Delta Delta C(T)) Method. Methods. 2001;25(4):402–8.
24. Wang W, Zhang T, Wu C, Wang S, Wang Y, Li H, et al. Immortalization of chicken preadipocytes by retroviral transduction of chicken TERT and TR. PLoS One. 2017;12(5):e0177348.
25. Shang Z, Guo L, Wang N, Shi H, Wang Y, Li H. **Oleate promotes differentiation of chicken primary preadipocytes in vitro**. Biosci Rep. 2014; 34(1).
26. Bolger AM, Lohse M, Usadel B. Trimmomatic: a flexible trimmer for Illumina sequence data. Bioinformatics. 2014;30(15):2114–20.
27. Kim D, Paggi JM, Park C, Bennett C, Salzberg SL. Graph-based genome alignment and genotyping with HISAT2 and HISAT-genotype. Nat Biotechnol. 2019;37(8):907–15.
28. Love MI, Huber W, Anders S. Moderated estimation of fold change and dispersion for RNA-seq data with DESeq2. Genome Biol. 2014;15(12):550.
29. Zhou Y, Zhou B, Pache L, Chang M, Khodabakhshi AH, Tanaseichuk O, et al. Metascape provides a biologist-oriented resource for the analysis of systems-level datasets. Nat Commun. 2019;10(1):1523.
30. Li R, Zhuang Y, Han M, Xu T, Wu X. piggyBac as a high-capacity transgenesis and gene-therapy vector in human cells and mice. Dis Model Mech. 2013;6(3):828–33.

31. Rao PK, Kumar RM, Farkhondeh M, Baskerville S, Lodish HF. Myogenic factors that regulate expression of muscle-specific microRNAs. Proc Natl Acad Sci U S A. 2006;103(23):8721–6.
32. Lv H, Sun Y, Zhang Y. MiR-133 is Involved in Estrogen Deficiency-Induced Osteoporosis through Modulating Osteogenic Differentiation of Mesenchymal Stem Cells. Med Sci Monit. 2015;21:1527–34.
33. Li Z, Hassan MQ, Volinia S, van Wijnen AJ, Stein JL, Croce CM, et al. A microRNA signature for a BMP2-induced osteoblast lineage commitment program. Proc Natl Acad Sci U S A. 2008;105(37):13906–11.
34. Ye N, Yang Y, Ma Z, Huang J. Ghrelin promotes the osteogenic differentiation of rMSCs via miR-206 and the ERK1/2 pathway. Cytotechnology. 2020;72(5):707–13.
35. Wang C, Liu W, Nie Y, Qaher M, Horton HE, Yue F, et al. Loss of MyoD Promotes Fate Transdifferentiation of Myoblasts Into Brown Adipocytes. EBioMedicine. 2017;16:212–23.
36. Jia X, Lin H, Abdalla BA, Nie Q. Characterization of miR-206 Promoter and Its Association with Birthweight in Chicken. Int J Mol Sci. 2016;17(4):559.
37. Birsoy K, Chen Z, Friedman J. Transcriptional regulation of adipogenesis by KLF4. Cell Metab. 2008;7(4):339–47.
38. Rivero S, Diaz-Guerra MJ, Monsalve EM, Laborda J, Garcia-Ramirez JJ. DLK2 is a transcriptional target of KLF4 in the early stages of adipogenesis. J Mol Biol. 2012;417(1–2):36–50.
39. Guo L, Cui H, Zhao G, Liu R, Li Q, Zheng M, et al. Intramuscular preadipocytes impede differentiation and promote lipid deposition of muscle satellite cells in chickens. BMC Genom. 2018;19(1):838.
40. Li F, Li Y, Duan Y, Hu CA, Tang Y, Yin Y. Myokines and adipokines: Involvement in the crosstalk between skeletal muscle and adipose tissue. Cytokine Growth Factor Rev. 2017;33:73–82.
41. Timmons JA, Wennmalm K, Larsson O, Walden TB, Lassmann T, Petrovic N, et al. Myogenic gene expression signature establishes that brown and white adipocytes originate from distinct cell lineages. Proc Natl Acad Sci U S A. 2007;104(11):4401–6.
42. Berkes CA, Tapscott SJ. MyoD and the transcriptional control of myogenesis. Semin Cell Dev Biol. 2005;16(4–5):585–95.
43. Choi J, Costa ML, Mermelstein CS, Chagas C, Holtzer S, Holtzer H. MyoD converts primary dermal fibroblasts, chondroblasts, smooth muscle, and retinal pigmented epithelial cells into striated mononucleated myoblasts and multinucleated myotubes. Proc Natl Acad Sci U S A. 1990;87(20):7988–92.
44. Li Y, Li F, Lin B, Kong X, Tang Y, Yin Y. Myokine IL-15 regulates the crosstalk of co-cultured porcine skeletal muscle satellite cells and preadipocytes. Mol Biol Rep. 2014;41(11):7543–53.
45. Kablar B, Krastel K, Tajbakhsh S, Rudnicki MA. Myf5 and MyoD activation define independent myogenic compartments during embryonic development. Dev Biol. 2003;258(2):307–18.
46. Borensztein M, Viengchareun S, Montarras D, Journot L, Binart N, Lombes M, et al. Double Myod and Igf2 inactivation promotes brown adipose tissue development by increasing Prdm16 expression. FASEB J. 2012;26(11):4584–91.
47. Petracci M, Cavani C. Muscle growth and poultry meat quality issues. Nutrients. 2012;4(1):1–12.
48. Sachs NJ, Hampton AR, Foster KK, Pechanec MY, Henderson JD, King AJ, et al. The effects of an alternative diet regimen with natural methionine ingredients on white striping breast myopathy in broiler

chickens. Poult Sci. 2019;98(1):413–21.

49. Hanna JA, Garcia MR, Go JC, Finkelstein D, Kodali K, Pagala V, et al. PAX7 is a required target for microRNA-206-induced differentiation of fusion-negative rhabdomyosarcoma. Cell Death Dis. 2016;7(6):e2256.
50. Keklikoglou I, Hosaka K, Bender C, Bott A, Koerner C, Mitra D, et al. MicroRNA-206 functions as a pleiotropic modulator of cell proliferation, invasion and lymphangiogenesis in pancreatic adenocarcinoma by targeting ANXA2 and KRAS genes. Oncogene. 2015;34(37):4867–78.
51. Sweetman D, Goljanek K, Rathjen T, Oustanina S, Braun T, Dalmay T, et al. Specific requirements of MRFs for the expression of muscle specific microRNAs, miR-1, miR-206 and miR-133. Dev Biol. 2008;321(2):491–9.
52. Gagan J, Dey BK, Layer R, Yan Z, Dutta A. Notch3 and Mef2c proteins are mutually antagonistic via Mkp1 protein and miR-1/206 microRNAs in differentiating myoblasts. J Biol Chem. 2012;287(48):40360–70.
53. Rosenberg MI, Georges SA, Asawachaicharn A, Analau E, Tapscott SJ. MyoD inhibits Fstl1 and Utrn expression by inducing transcription of miR-206. J Cell Biol. 2006;175(1):77–85.
54. Tang R, Ma F, Li W, Ouyang S, Liu Z, Wu J. **miR-206-3p Inhibits 3T3-L1 Cell Adipogenesis via the c-Met/PI3K/Akt Pathway**. Int J Mol Sci. 2017; 18(7).
55. Chen QY, Jiao DM, Wu YQ, Chen J, Wang J, Tang XL, et al. MiR-206 inhibits HGF-induced epithelial-mesenchymal transition and angiogenesis in non-small cell lung cancer via c-Met /PI3k/Akt/mTOR pathway. Oncotarget. 2016;7(14):18247–61.
56. Zhang YY, Li X, Qian SW, Guo L, Huang HY, He Q, et al. Transcriptional activation of histone H4 by C/EBPbeta during the mitotic clonal expansion of 3T3-L1 adipocyte differentiation. Mol Biol Cell. 2011;22(13):2165–74.
57. Guo L, Li X, Huang JX, Huang HY, Zhang YY, Qian SW, Zhu H, et al. Histone demethylase Kdm4b functions as a co-factor of C/EBPbeta to promote mitotic clonal expansion during differentiation of 3T3-L1 preadipocytes. Cell Death Differ. 2012;19(12):1917–27.

Figures

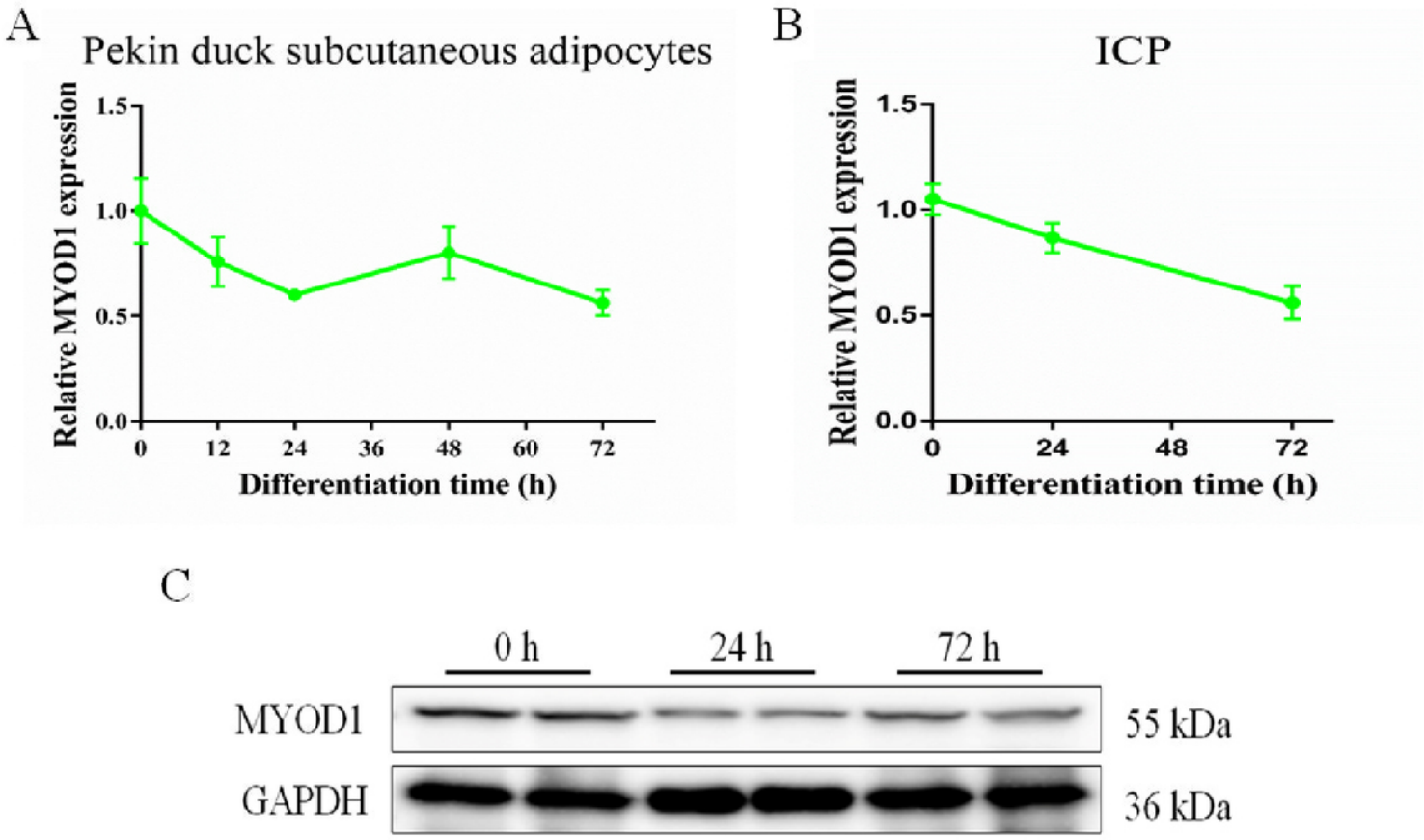

Figure 1

MYOD1 is down-regulated in the early stage of avian adipocyte differentiation. (a, b) MYOD1 mRNA levels in different time points during the differentiation of Pekin duck subcutaneous preadipocytes (mRNA-Seq) and ICPs (qPCR). (c) MYOD1 protein levels at different time points during ICPs differentiation were determined by Western blotting.

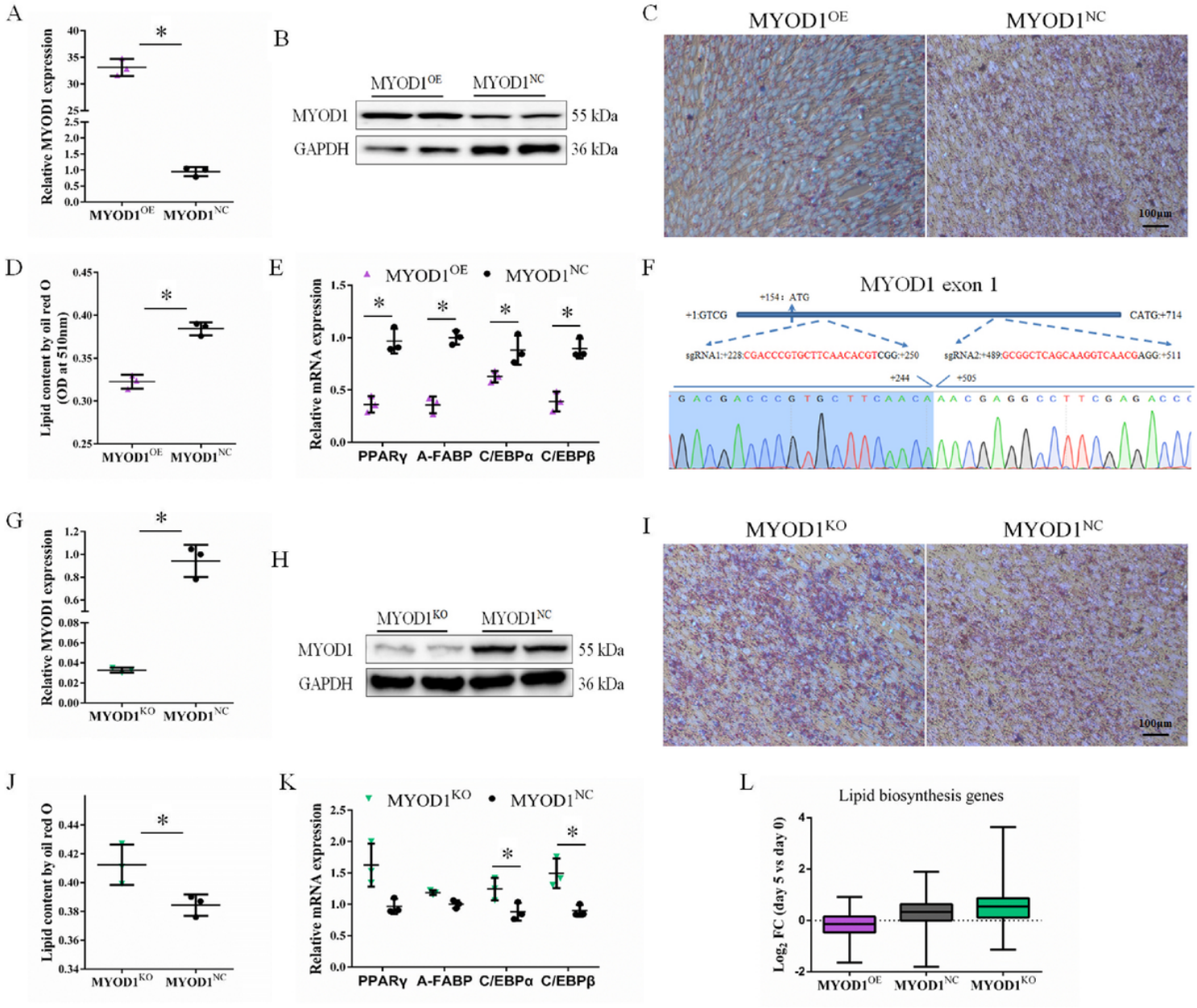

Figure 2

MYOD1 is a repressor of avian adipocyte differentiation. (a, b) MYOD1OE cell significantly promoted MYOD1 mRNA and protein expression in ICPs. (c) Representative images of MYOD1OE cells reduced the lipid droplet formation by Oil Red O staining on day 3. (d) Comparison of the lipid droplet content of MYOD1OE and MYOD1NC cells obtained by oil red O staining and extraction methods. (e) mRNA levels of adipocyte genes PPARγ, A-FABP, C/EBPα, and C/EBPβ were analyzed with qPCR. (f) Upper part: schematic diagram of MYOD1 exon1 region and the two targeting loci of MYOD1 sgRNA (red). Lower part: DNA sequence map around the targeting locus of the cleaved band amplified from ICPs transfected with both sgRNAs. (g, h) MYOD1KO significantly reduced MYOD1 mRNA and protein expression in ICPs. (i) Representative images of MYOD1KO cells promoted the lipid droplet formation by Oil Red O staining on day 3. (j) Comparison of the lipid droplet content of MYOD1OE and MYOD1NC cells obtained by oil red O staining and extraction methods. (k) mRNA levels of adipocyte marker genes were analyzed with qPCR. (l) Compare the fold change of known lipid biosynthesis genes in MYOD1OE, MYOD1NC, and MYOD1KO cells on day 5 compared to day 0. Data are

shown as mean ± SD of three biological replicates. Three independent sample t-test was used to analyze the statistical differences between groups. *, P ⍰ 0.05.

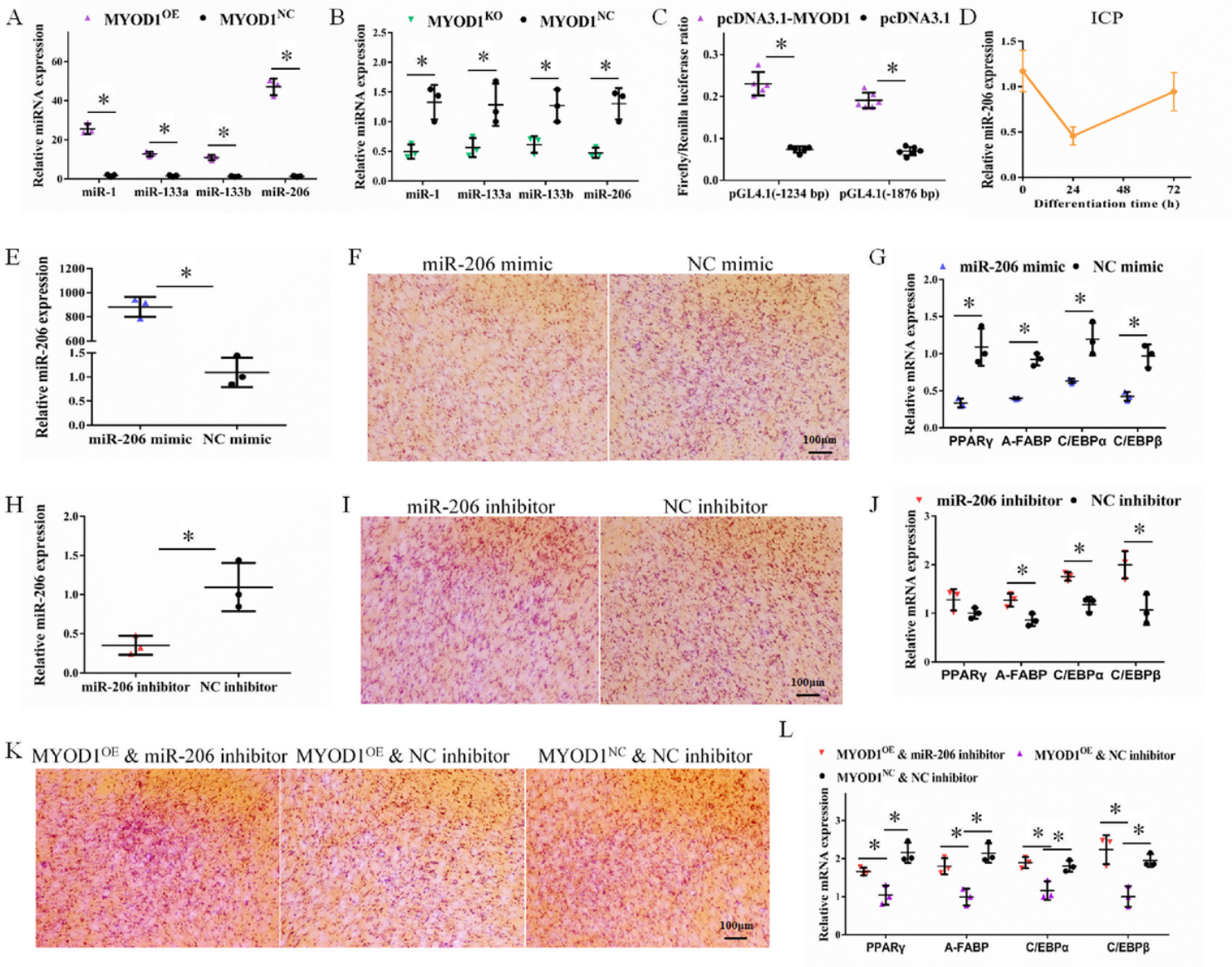

Figure 3

The inhibitory effect of MYOD1 on adipocyte differentiation was achieved by its downstream gene miR-206. (a) over-expression of MYOD1 up-regulated miR-1, miR-133a, miR-133b, and miR-206 expression in ICPs. (b) MYOD1 knockout down-regulated miR-1, miR-133a, miR-133b, and miR-206 expression in ICPs. (c) MYOD1 over-expression promoted the relative luciferase activity of the pGL4.1 (−1234 bp) and pGL4.1(−1876 bp) reporter in ICPs. (d) Relative miR-206 expression during ICPs differentiation. (e) Transfected with miR-206 mimic significantly promoted miR-206 expression in ICPs. (f) Over-expression of miR-206 reduced the lipid droplet formation by Oil Red O staining on day 3. (g) mRNA levels of adipocyte marker genes were analyzed with qPCR. (h) Transfected with miR-206 inhibitor significantly reduced miR-206 expression in ICPs. (i) Inhibition of miR-206 promoted the lipid droplet formation by Oil Red O staining on day 3. (j) mRNA levels of adipocyte marker genes were analyzed with qPCR. (k) Inhibition of miR-206 could counteract the inhibition effect of MYOD1 over-expression on adipocyte differentiation. (l) mRNA levels of adipocyte marker genes

were analyzed with qPCR. Data are shown as mean ± SD of three biological replicates. Three independent sample t-test was used to analyze the statistical differences between groups. *, P ⍰ 0.05.

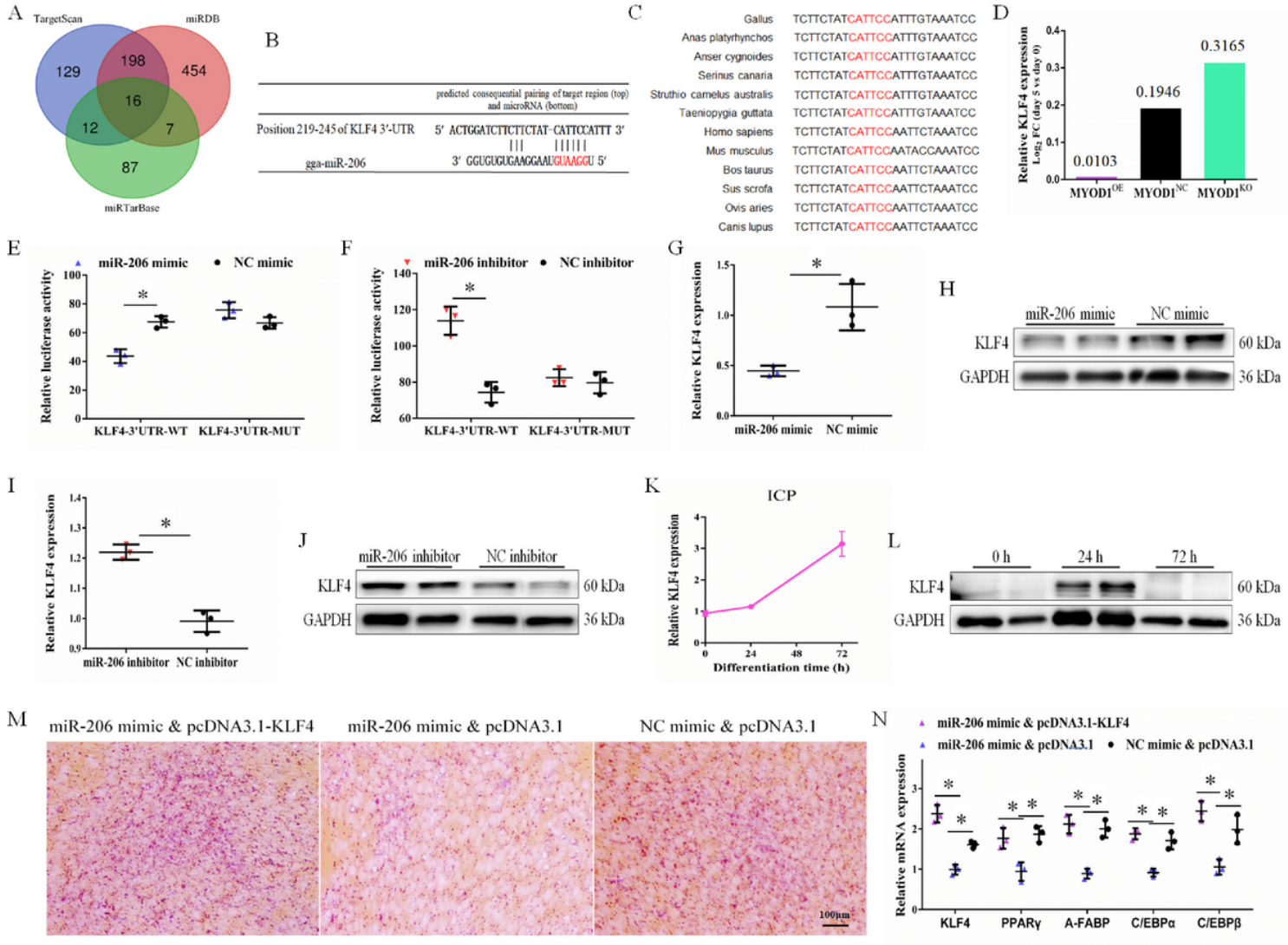

Figure 4

KLF4 is the miR-206 target gene, functioning as an activator of adipocyte differentiation. (a) Overlap of three miRNA target bioinformatic prediction algorithms. (b) The potential binding site of miR-206 in the KLF4 mRNA 3'-UTR. (c) The potential binding site (red) of miR-206 in the KLF4 mRNA 3' -UTR is highly conserved among vertebrates. (d) Compare the fold change of KLF4 in MYOD1OE, MYOD1NC, and MYOD1KO cells at day 5 compared to day 0. (e, f) Dual-luciferase reporter assay indicated that miR-206 could bind to the predicted binding site of the KLF4 mRNA 3'-UTR. (g, h) miR-206 over-expression inhibited KLF4 mRNA and protein expression in ICPs. (i, j) miR-206 inhibition promoted KLF4 mRNA and protein expression in ICPs. (k, l) KLF4 mRNA and protein levels at different time points during ICPs differentiation. (m) Over-expression of KLF4 could counteract the inhibition effect of miR-206 over-expression on adipocyte differentiation. (n) mRNA levels of adipocyte marker genes were analyzed with qPCR. Data are shown as mean ± SD of three biological replicates. Three independent sample t-test was used to analyze the statistical differences between groups. *, P ⍰ 0.05.

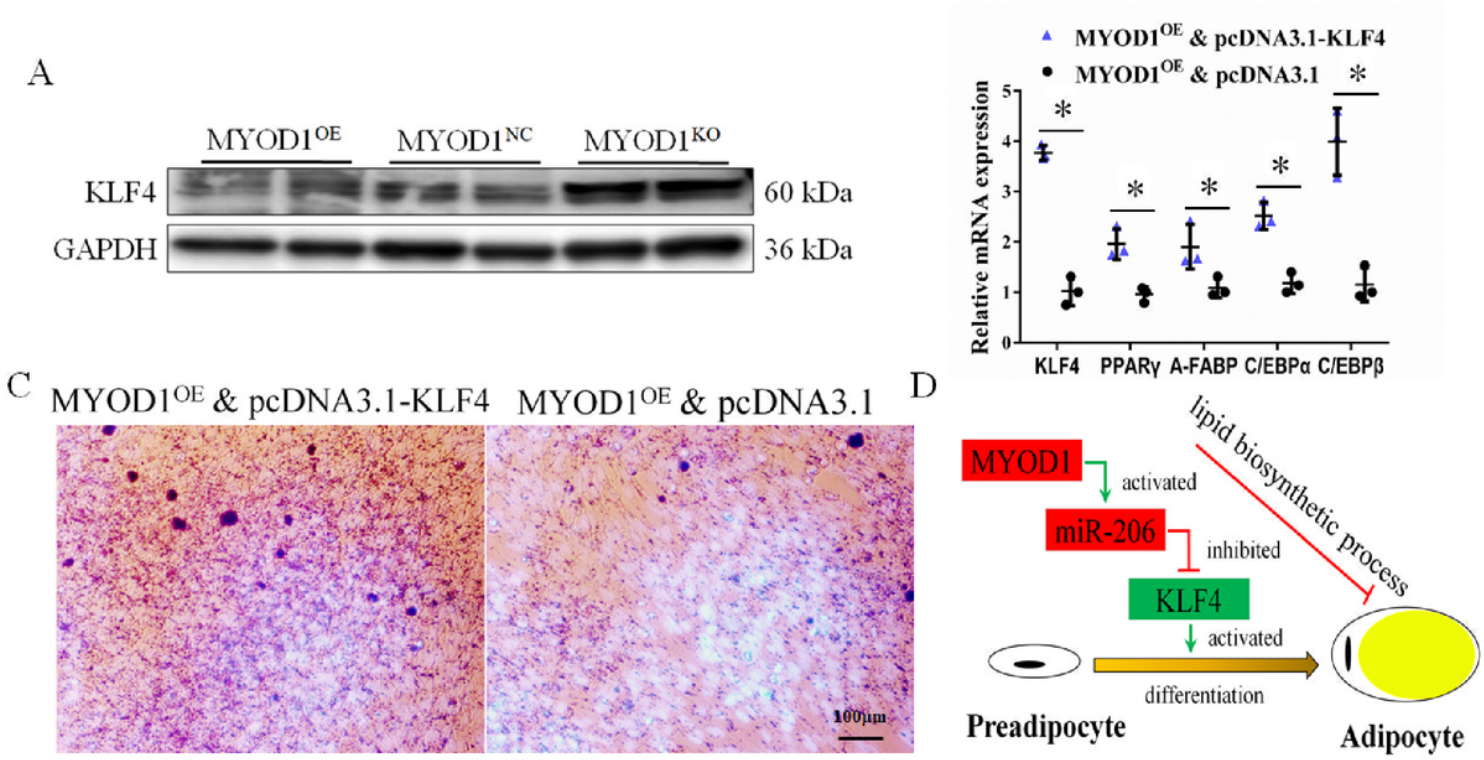

Figure 5

MYOD1 affected KLF4 expression. (a) Western blot analysis of the protein levels of KLF4 in MYOD1OE, MYOD1NC, and MYOD1KO cells. (b) mRNA levels of adipocyte marker genes were analyzed with qPCR. (c) Representative images of KLF4 over-expression promoted the lipid droplet formation by Oil Red O staining (red). (d) Model of the MYOD1-mediated regulatory pathway for adipocyte differentiation. Data are shown as mean ± SD of three biological replicates. Three independent sample t-test was used to analyze the statistical differences between groups. *, P □ 0.05.

Supplementary Files

This is a list of supplementary files associated with this preprint. Click to download.

- FigureS1.tif
- SupplementaryInformation.docx
- Tab.S1.xlsx
- Tab.S2.xlsx
- Tab.S3.xlsx
- Tab.S4.xlsx
- Tab.S5.xlsx
- Tab.S6.xlsx
- Tab.S7.xlsx
- Tab.S8.xlsx

- Tab.S9.xlsx